Neurochemical Research (2019) 44:2577–2589
https://doi.org/10.1007/s11064-019-02876-4

ORIGINAL PAPER

PKCγ and PKCε are Differentially Activated and Modulate Neurotoxic Signaling Pathways During Oxygen Glucose Deprivation in Rat Cortical Slices

Dayana Surendran[1]

Received: 18 May 2019 / Revised: 10 September 2019 / Accepted: 13 September 2019 / Published online: 20 September 2019

Abstract

Cerebral ischemia is known to trigger a series of intracellular events such as changes in metabolism, membrane function and intracellular transduction, which eventually leads to cell death. Many of these processes are mediated by intracellular signaling cascades that involve protein kinase activation. Among all the kinases activated, the serine/threonine kinase family, protein kinase C (PKC), particularly, has been implicated in mediating cellular response to cerebral ischemic and reperfusion injury. In this study, using oxygen–glucose deprivation (OGD) in acute cortical slices as an in vitro model of cerebral ischemia, I show that PKC family of isozymes, specifically PKCγ and PKCε are differentially activated during OGD. Detecting the expression and activation levels of these isozymes in response to different durations of OGD insult revealed an early activation of PKCε and delayed activation of PKCγ, signifying their roles in response to different durations and stages of ischemic stress. Specific inhibition of PKCγ and PKCε significantly attenuated OGD induced cytotoxicity, rise in intracellular calcium, membrane depolarization and reactive oxygen species formation, thereby enhancing neuronal viability. This study clearly suggests that PKC family of isozymes; specifically PKCγ and PKCε are involved in OGD induced intracellular responses which lead to neuronal death. Thus isozyme specific modulation of PKC activity may serve as a promising therapeutic route for the treatment of acute cerebral ischemic injury.

Keywords Cerebral ischemia · Oxygen glucose deprivation (OGD) · Protein kinase C (PKC) · Intracellular calcium ($[Ca^{2+}]_i$) · Membrane potential · Reactive oxygen species (ROS)

Introduction

Cerebral ischemia is a leading cause of death and also the most common cause of long- term disability worldwide. It is known to trigger a series of destructive cellular processes including excitotoxicity, spreading depolarization, changes in metabolism, membrane function, inflammation and blood–brain barrier breakdown, which eventually lead to cell injury/death. Many of these processes are mediated by intracellular signaling cascades that involve protein kinase activation [1–3]. In particular, protein kinase C (PKC) has been believed to play a crucial role in mediating cellular responses to cerebral ischemia, as PKCs are extensively expressed in the brain, and are involved in a myriad of cellular processes; both physiological and pathological, such as neurotransmitter release, ion homeostasis, synaptic plasticity, plasma membrane failure, apoptosis etc. [4–6].

Protein kinase C (PKC), a family of 10 phospholipid-dependent serine-threonine kinases are divided into three groups: conventional (PKC-α, βI, βII and γ), novel (PKC-δ, ε, η and θ) and atypical (PKC ι/λ and ς), based on their structure and co-factor requirements for activation. The conventional isoforms are activated by calcium (Ca^{2+}) and diacylglycerol (DAG) or phorbol ester, the novel isoforms by DAG or phorbol ester, but are calcium independent, and the atypical PKC isoforms which are not activated by DAG, phorbol ester, or Ca^{2+}. When activated, PKCs translocate from the soluble cytosolic fraction to cellular membranes, where they then interact with anionic phospholipids [7] like

Electronic supplementary material The online version of this article (https://doi.org/10.1007/s11064-019-02876-4) contains supplementary material, which is available to authorized users.

✉ Dayana Surendran
dayana.surendran@gmail.com

[1] Department of Biophysics, National Institute of Mental Health and Neurosciences, Bengaluru 560 029, India

DAG, and are properly localized by receptors for activated C kinase (RACKs) to phosphorylate neighboring protein substrates [8]. PKC isozyme activity has been reported during ischemic injury in several tissues like the cardiac, hepatic and renal [9–11]. The involvement of PKCs in the chain of events following cerebral ischemia is debatable due to varied reports [12, 13]. Some studies report that total PKC levels and activity increase at very early time points following ischemia in an in vivo model [14, 15]. Inhibition of PKC using non-specific PKC inhibitors such as H7, calphostin C, or staurosporin, defends against excitotoxic cell death induced by nitric oxide, anoxia or glutamate in vitro [16, 17] and against ischemic damage in vivo [18]. However, majority of the studies have reported a loss in PKC activity and expression following ischemia implicating PKC is down-regulated/degraded [19, 20]. A total loss in PKC activity is also reported to be observed in in vitro culture models of ischemic and excitotoxic cell death [21, 22]. These conflicting reports from previous studies may arise from the use of different ischemic models, activation factors, cell types, duration and intensities of ischemic insult and the use of non-specific pharmacological tools. Moreover, the fact that individual PKC isoforms mediate different and sometimes opposing actions even after being activated by the same stimulus [23] could also have contributed to these controversial results. However, the exact role of individual PKC isozymes as positive or negative modulators of ischemic neuronal damage has been unclear but might include multiple cellular machineries. In the present communication, I investigated the role of PKC isozymes in mediating neuronal signaling pathways during oxygen glucose deprivation (OGD), an in vitro model for cerebral ischemia, in rat cortical slices.

Materials and Methods

Materials

Fura-2 acetoxy methyl ester (Fura-2-AM; Cat# F1221), Rhodamine123 (Rh123; Cat# R8004), 2′7′- dichlorodihydro fluorescein diacetate (H2DCF-DA; Cat# D6883) and pluronic F-127 (Cat# P6867) were obtained from Molecular Probes Inc. (Eugene, OR, USA). Protein kinase C epsilon (PKC-ε; Cat# sc-1681)), protein kinase C gamma (PKC-γ; Cat# sc-166385)), β-actin (Cat# sc-47778) antibodies were procured from Santa Cruz, USA. Carbonyl cyanide 3-chlorophenylhydrazone (CCCP), chelerythrine chloride (Cat# C2932), ethylene glycol-bis (2-aminoethylether)-*N*,*N*,*N*′′,*N*′′-tetraacetic acid (EGTA), aprotinin, leupeptin, pepstatin, sodium orthovanadate, phenylmethanesulfonyl fluoride (PMSF), acrylamide, dithiothreitol (DTT), sodium fluoride (NaF) and horse-radish peroxide antibody (goat-antirabbit; Cat# AP132P) were purchased from Sigma Aldrich, India. Cell-permeable myristoylated translocation peptide inhibitors specific for PKCγ (Myr-RLVLAS-OH) and PKCε ((Myr-EAVSLKPT-OH) were custom synthesized by Imgenex Pvt. Ltd, Bhubaneshwar, Odisha, India. Supersignal® West Pico chemiluminiscent substrate was procured from Pierce, Rockford, USA). Immobilon® Polyvinyledene difluoride (PVDF) membrane was purchased from Millipore, USA). Horse-radish peroxide antibody (goat-antimouse; Cat# 1140680011730) was obtained from Bangalore Genei, Bengaluru. All other chemicals were of analytical grade obtained from commercial sources.

Preparation of Rat Cortical Slices

Animals were obtained from the Central Animal Research Facility (CARF) of National Institute of Mental Health and Neurosciences, Bengaluru, India. All experimental protocols and procedures were performed in accordance with the guidelines set by the Institutional Animal Ethics Committee (IAEC) for the care and use of animals for experimental work. Animals were housed in polypropylene cages and they had access to pelleted diet and water ad libitum. Adult male Sprague–Dawley rats aged 2 months were used throughout the study. Acute cerebral cortical slices prepared from the parietal region were used as the experimental system. A total of 45 rats were used for this study. Briefly, rats were sacrificed by cervical dislocation; decapitated and whole brains were rapidly removed and placed in ice-cold high sucrose buffer (composition in mM: 215 Sucrose, 2.5 KCl, 10 D-Glucose, 3.3 $MgSO_4$, 0.5 $CaCl_2$, 26.2 $NaHCO_3$, 1.13 ascorbate; pH 7.4; 310–320 mOsm/L). 15–20 sagittal cortical slices of 350 µm thickness were prepared from either hemisphere from the parietal region of the cerebrum using a vibratome (The Vibratome Company, USA). The tissue remained submerged in ice-cold high sucrose buffer for minimal damage during slice preparation. Individual slices were trimmed to separate the sub-cortical structures from the cortical region. Subsequently the slices were incubated in Kreb's Hensleit (KH) buffer [artificial cerebrospinal fluid (aCSF)] (124 mM NaCl, 5 mM KCl, 1.2 mM MgSO4, 1.2 mM CaCl2, 23 mM NaHCO3, 1.2 mM KH2PO4, HEPES and 10 mM D-Glucose; pH 7.4, 300–305 mOsm) that was continuously equilibrated with 95% O_2 and 5% CO_2 at room temperature for 60 min to achieve complete metabolic recovery. The viability of the slices was assessed by measuring the percentage of dissolved oxygen (%DO_2) consumption using a Clark's type polarographic dissolved oxygen meter (JENWAY Ltd, U.K). The DO_2% of the buffer at different time points (0 min, 5 min, 15 min, 30 min, 60 min and 120 min) was measured using a dissolved oxygen meter. In normoxic group, the initial DO_2% was above 40%, which is well above the mean pO_2 in arterial blood. The DO_2% in normoxic group after 120 min was

found to be almost 20–21%, which is equivalent to 142.75 mm of Hg. This is equal to the mean pO_2 in arterial blood. This is a clear indication that the prepared slices maintained viability till 120 min. A total of 45 rats were used for this study.

Generation of Ischemic stress In-Vitro

Oxygen–glucose deprivation (OGD) was used as in vitro model for cerebral ischemia. Percentage of dissolved oxygen (DO_2%) has been used as a measure of ischemia. Following metabolic recovery, I divided the slices into 2 groups: normoxic and oxygen-glucose deprived (ischemic). The normoxic group slices (4–5 slices) were transferred to aCSF containing glucose pre-equilibrated with 95% O_2 and 5% CO_2. For inducing ischemia (OGD), 4–5 slices were transferred to aCSF lacking glucose and pre-equilibrated with 95% N_2 and 5% CO_2. Glucose was substituted with equimolar concentration of sucrose to maintain osmolarity. For maintaining ischemic conditions, the aCSF containing slices was continuously bubbled with 95% N_2 and 5% CO_2 at a rate of ~ 2 L/min. Since my aim was to examine the time-course of the development of cerebral ischemia, so as to identify the underlying pathophysiological mechanisms, the DO_2% of aCSF at different time points (in minutes: 0, 5, 15, 30, 60 and 120) was measured using a Clark's type polarographic dissolved oxygen sensor. In normoxic group the initial DO_2% was above 40%, which is well above the mean pO_2 in arterial blood. The DO_2% in normoxic group after 120 min was found to be almost 20–21%, which is equivalent to 142.75 mm of Hg. This is equal to the mean pO_2 in arterial blood. In OGD groups the DO_2% was found to be less than 2.1% after equilibrating the aCSF with 95% N_2 and 5% CO_2 for 30 min which is equal to 14.97 mm of Hg which is well within the generally accepted limit for in vivo hypoxia. 4–5 slices were used for each time point/group/experiment. Once the model was established, the slices were exposed to the given experimental conditions.

Lactate Dehydrogenase Assay

Cell death was quantified by measuring lactate dehydrogenase (LDH) released from the slices into the extracellular medium. Cytotoxicity under the above set of experimental conditions was estimated by measuring the LDH released from the slices. 200 µL aliquots of aCSF were collected from both normoxic and OGD groups at different time points (0, 5, 15, 30, 60 and 120 min) for measuring the extent of cell death. 4/5 slices were used for each time point/group/experiment. LDH activity was determined by monitoring the change in optical density (ΔO.D) or absorbance of NADH at 340 nm for 3 min at room temperature using UV–Vis spectrophotometer (Labomed, USA). The total protein content in the particulate fractions was estimated by *Lowry's* method. LDH release at the above time points was normalized against total protein content and the specific activity was expressed as ΔO.D at 340 nm/min/g of protein [24].

Isolation of particulate fractions

Slices after respective treatment were stored in hypotonic lysis buffer (composition in mM; 25 HEPES, 0.3 NaCl, 0.2 EDTA, 0.05 dithiothreitol, 20 NaF, 1 PMSF, 1.5 $MgCl_2$, 0.1 sodium orthovanadate, 0.025 mM aprotinin, 0.05 mM leupeptin, 0.05 mM pepstatin; pH 7.6) and frozen until analysis. For Western blot analysis, the slices were homogenized in hypotonic lysis buffer using Dounce homogenizer. The particulate fractions were isolated as described in [25] with minor modifications. Briefly, the homogenate was centrifuged at 1000×*g* at 4 °C for 10 min. The supernatant was carefully taken off and re-centrifuged at 16,000×*g* for 15 min. The pellet was re-suspended in lysis buffer containing 0.1% Triton X-100 and was referred to as the 'particulate' fraction. The particulate fractions were evaluated for protein content by *Lowry's* method.

Western Blot Analysis

Equal amounts (40 µg) of protein from normoxic and OGD groups at 0, 5, 15, 30, 60 and 120 min time points were separated by 10% SDS-PAGE and then transferred to PVDF membrane using a semi-dry electro blotting apparatus (Atto Corporation, Japan). After blocking in Tris-buffered saline with 0.1% (v/v) Tween-20 (T-TBS) and 5% non-fat dry milk at 4 °C overnight, the membrane was incubated for 2 h with primary antibodies: anti-rabbit-protein kinase C gamma (PKC-γ), protein kinase C epsilon (PKC-ε) and anti-mouse β-actin (PKC-γ at 1:1000, PKC-ε at 1:500 and β-actin at 1:1000 dilution respectively) at room temperature. The membrane was then washed with T-TBS followed by incubation with appropriate secondary antibody (HRP-GAM at 1:2000 and HRP-GAR at 1:1000 dilutions respectively) for 1 hour. β-actin expression was determined as an internal control. Immunoreactivity was detected using enhanced chemiluminiscence which was visualized using a camera attached to a computer assisted gel documentation system (Syngene, UK) and the band densities were quantified by the Image J software (NIH).

Intracellular Calcium $[Ca^{2+}]_i$ Measurements

Intracellular calcium $[Ca^{2+}]_i$ measurements were performed using a fluorescence spectrophotometer (SLM-AMINCO-Bowman Series 2, Spectronic Instruments, SPECTRONIC UNICAM, Rochester, NY, USA) using the ratiometric calcium indicator dye Fura-2 AM. Briefly, metabolically

recovered slices were incubated for 1 hour in aCSF containing Fura-2 AM at a final concentration of 7.5 μM with 0.08% pluronic F-127 at 30–31 °C. With minor modifications to the cuvette-based fluorescence measurement method described in [26], after de-esterification of the dye, each slice was mounted on a rectangular glass cover slip and the top and bottom portions of the slice were fastened using thin strips of parafilm for support without inflicting any damage, with both sides of the slice in contact with aCSF. The cover slip was then placed diagonally into a fluorometer quartz cuvette in such a way that the incident beams could fall well within the slice area at an angle of 45°. The cover slip was held in position using a cuvette lid with a diagonal cut (Fig. S1). Normoxic and OGD experiments were carried out as mentioned above. For maintaining OGD conditions in the cuvette it was sealed and continuously flushed with 95% N_2 and 5% CO_2 at a rate of 2 L/min throughout the entire experimental duration. Background fluorescence from unloaded slices under my experimental conditions was determined and subtracted from total fluorescence prior to calculation of $[Ca^{2+}]_i$ (Fig. S2). The dye-loaded slice was alternately excited at 340 nm and 380 nm respectively and relative changes in $[Ca^{2+}]_i$ were expressed as change in the ratio of 340/380 nm fluorescence emission at 500 nm. The change in fluorescence intensity ratio was monitored for 30 min duration (Fig. S3). After 30 min of OGD exposure, a sharp decrease in both 340 nm and 380 nm individual traces were observed during fluorescence measurements. This could possibly be due to dye leakage into the extracellular medium from the slices. This may suggest an inability of the slices to retain the dye as a result of compromised cytoarchitecture upon continuous OGD exposure. Hence the fluorescence intensity changes were monitored only till 30 min.

Mitochondrial Membrane Potential Measurements

Mitochondrial membrane potential ($\Delta\Psi m$) changes were monitored using the voltage-sensitive fluorescent probe Rh123. The slices were incubated with Rh123 (2 μM) in aCSF for 20 min at 30 °C and fluorescence measurements were performed as mentioned earlier. The dye was maintained at a concentration of 0.5 μM in the cuvette during measurements to maintain its equilibrium distribution and to compensate for dye leakage irrespective of changes in plasma membrane potential. Normoxic and OGD experiments were carried out as mentioned above. Temporal changes in Rh123 fluorescence intensity (F) at 537 nm were normalized to the basal fluorescence intensity (F_0). The fluorescence was recorded for up to 30 min. Fluorescence intensity changes were monitored only till 30 min due to the reasons mentioned above. At the end of the experiments, CCCP (1 μM) was added to the slices to determine the specificity of Rh123 to mitochondrial membrane potential (Fig. S4). 1–2 slices/group/experiment from a total of 5 animals were used for this experiment.

Reactive Oxygen Species (ROS) Formation Measurements

The rate of ROS formation was measured using the oxidation sensitive fluorescent probe 2′7′-dichlorodihydrofluorescein diacetate (H_2DCF-DA). In brief, the slices were incubated with 100 μM of H_2DCF-DA for 40 min at room temperature. After de-esterification the slices were mounted on a rectangular glass cover slip as described elsewhere. The slices were excited at 495 nm and H_2DCF-DA fluorescence intensity changes in response to normoxia and OGD were monitored at 530 nm for 30 min. Normoxic and OGD experiments were carried out as mentioned earlier. The fluorescence intensity (F) at a given time point was normalized to the baseline fluorescence intensity (F0) and represented as normalized DCF fluorescence. 1–2 slices/group/experiment from a total of 5 animals were used for this study.

Statistical Analysis

All results are expressed as mean ± SEM. Statistical evaluation of the data was performed using Student's *t* test or one-way analysis of variance with Bonferroni's test. $P < 0.05$ was considered significant.

Results

OGD Induces Cell Death in Rat Cortical Slices

Previous studies have reported that the pathways activated and cellular and molecular processes initiated at different time points of ischemic insult were relatively different. To determine the time dependent effect of normoxia and ischemia on slice viability, I measured the lactate dehydrogenase (LDH) released into the extracellular medium at 0, 5, 15, 30, 60 and 120 min by measuring the absorbance of NADH at 340 nm using UV–Vis spectrophotometer. Under normoxic conditions, there is a slow and steady rise in LDH release from cortical slices for up to 120 min suggesting slices were viable but showed a time dependent gradual decrease in slice viability. I found a significant increase in LDH release from 15 min (1.44 fold) onwards in slices exposed to in vitro ischemic conditions (OGD) and at 120 min a maximal increase of 3.65 fold was observed as compared to normoxic slices with same duration of exposure (Fig. 1a).

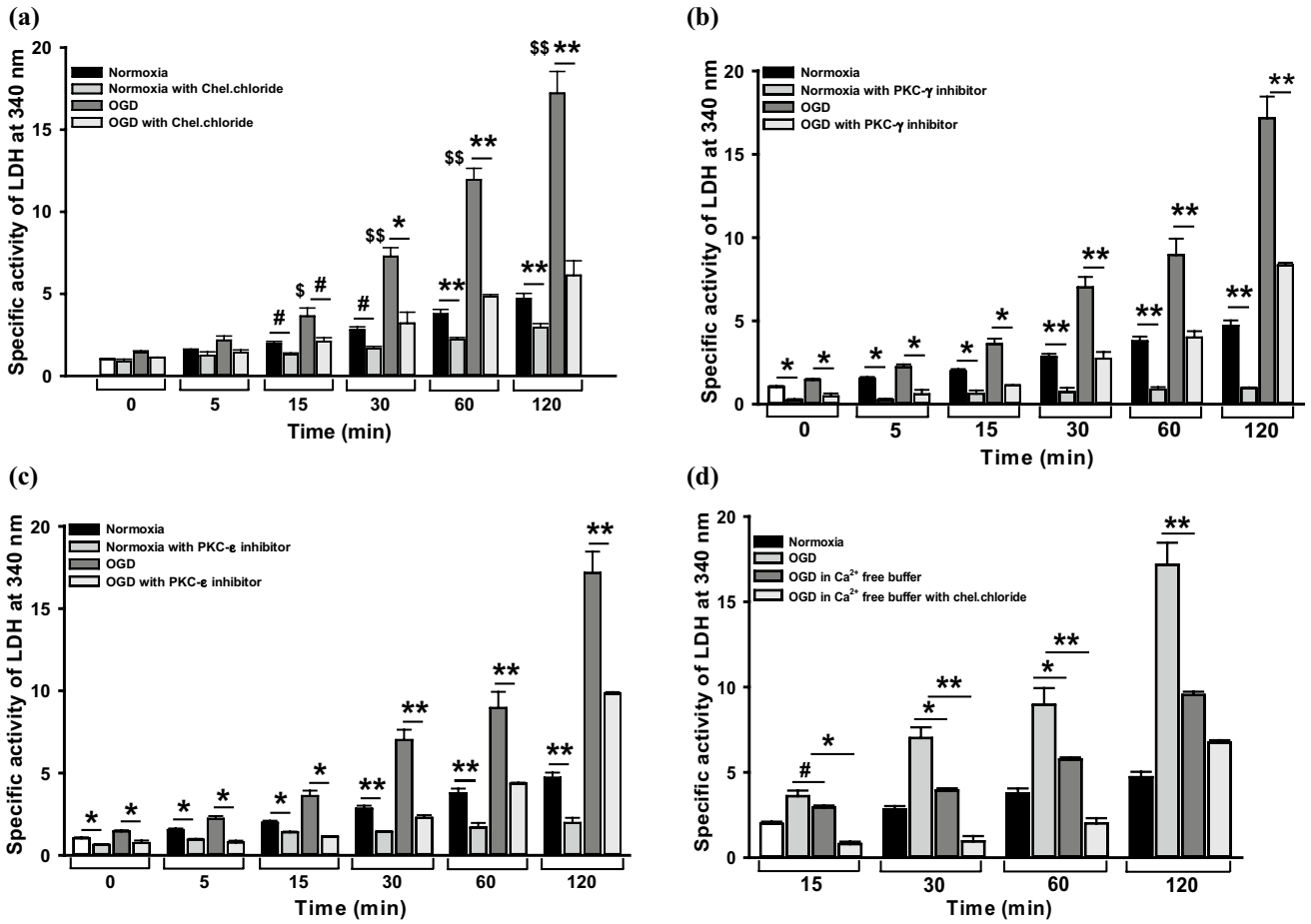

Fig. 1 Comparative study of lactate dehydrogenase (LDH) release assay. **a** (i) LDH release under normoxic and oxygen glucose deprivation (OGD) for different time durations of 0, 5, 15, 30, 60 and 120 min. Data presented as mean ± SEM from 6 different experiments.$ $P < 0.05$,$$ $P < 0.001$ observed between normoxic and OGD groups. ii) Effect of chelerythrine chloride (10 μM) on OGD-induced cytotoxicity. Data presented are mean ± SEM from 4 different experiments. *$P < 0.05$, #$P < 0.01$, **$P < 0.001$ between OGD and OGD with chelerythrine chloride pre-treatment groups. *$P < 0.05$ normoxia versus normoxia with chelerythrine chloride and OGD and OGD with chelerythrine chloride respectively. **b** Effect of PKC-γ specific peptide inhibitor ((10 μM) on OGD-induced cytotoxicity. Data presented are mean ± SEM from 4 different experiments. *$P < 0.005$ and **$P < 0.001$ between normoxic versus normoxia with PKC-γ inhibitor pre-treated groups and OGD versus OGD with PKC-γ inhibitor pre-treated groups. **c** Effect of PKC-ε specific peptide inhibitor (10 μM) on OGD-induced cytotoxicity. Data presented are mean ± SEM from 4 different experiments. *$P < 0.005$ and **$P < 0.001$ between normoxic versus normoxia with PKC-ε inhibitor pre-treated groups and OGD versus OGD with PKC-ε inhibitor pre-treated groups. **d** Effect of extracellular calcium on OGD-induced LDH release. Data presented are mean ± SEM from 3 different experiments. #$P < 0.05$, *$P < 0.005$ and **$P < 0.001$ between OGD, OGD in calcium-free aCSF and OGD in calcium-free aCSF with chelerythrine chloride pre-treated groups

PKC Inhibitors Attenuate OGD Induced Cell Death

Since OGD exposure caused significant cell death in cortical slices, I sought to determine the overall effect of PKC family of isozymes on OGD induced cytotoxicity. For this, I used both general PKC inhibitors and inhibitors specific for PKC-ε and PKC-γ. The slices were pre-treated with the general PKC inhibitor chelerythrine chloride (10 μM for 15 min) in KH buffer, and the LDH released into the extracellular medium at the above time points was measured. The LDH release was significantly lower even in chelerythrine chloride pre-treated normoxic slices compared to untreated normoxic slices. I observed that pre-treatment with chelerythrine chloride attenuated OGD induced LDH release by 34.38 ± 4.23, 42.17 ± 6.23%, 55.90 ± 8.16%, 59.63 ± 6.08 and 64.38 ± 10.2% at 5, 15, 30, 60 and 120 min respectively (Fig. 1a). This suggests that overall activity of PKC family of isozymes is deleterious to neuronal survival during OGD.

Since the cytotoxicity experimental data with general PKC inhibitor indicated that PKC activity contributes substantially towards OGD induced toxicity, I further evaluated the involvement of PKC-γ, which is expressed exclusively in brain and PKC-ε, which is reported to be involved in ischemic preconditioning in the brain, in the observed

toxicity. The activity of PKC-γ isozyme was inhibited by utilizing isozyme specific myristoylated hexa-peptide inhibitor, myr-RLVLAS-OH (10 μM for 30 min) in KH buffer. This cell permeable peptide derived from the C2 domain of PKC-γ is isozyme-selective and competes with activated PKC-γ for binding to γ –RACK thus inhibiting its function [27]. I found that PKC-γ inhibition during OGD insult led to a significant inhibition in LDH release from 5 min (73.38 ± 4.37%) onwards (Fig. 1b). The maximal inhibition in LDH release was observed at 30 min (75.74 ± 10.29%) and after 60 min of OGD the protective effect of the peptide inhibitor starts to decline. I next determined the effects of PKC-ε isozyme inhibition on OGD-induced neuronal death in cortical slices using the PKC-ε selective inhibitor peptide, myr-EAVSLKPT-OH (10 μM for 30 min) in KH buffer. This octapeptide is a cell permeable myristoylated translocation inhibitor peptide of PKC-ε [28] that selectively inhibits PKC-ε in a reversible manner. PKC-ε inhibition during OGD insult resulted in a marked reduction (64.64%) in LDH release from 5 min onwards (Fig. 1c). The inhibition levels remained almost stable till 30 min and start to decrease from 60 min onwards.

OGD-Induced Cytotoxicity is Ca^{2+}-Dependent

To determine whether OGD induced neurotoxicity is calcium-dependent; I next assessed the extent of LDH release in calcium-free aCSF as compared to calcium containing conditions. Slices exposed to OGD in calcium free aCSF containing 1 mM EGTA showed a significant reduction in LDH activity compared to slices exposed to OGD in calcium containing aCSF (Fig. 1d). Since I observed a significant decrease in LDH release in chelerythrine chloride pre-treated OGD slices from 15 min onwards I chose the time points 15 min, 30 min, 60 min and 120 min for this experiment. The LDH release at the end of 120 min in OGD slices under calcium free conditions was found to be 44.58% lesser as compared to slices in calcium containing conditions, indicating that calcium influx is a major contributing factor in OGD induced cytotoxicity.

I further investigated the role of calcium independent PKC isozymes in OGD induced cytotoxicity. Slices were pre-treated with chelerythrine chloride (10 μM) and the LDH activity in calcium free aCSF was measured. Chelerythrine chloride pre-treated slices showed a significant reduction (50.85 ± 7.15%) in LDH release till 60 min of OGD exposure (Fig. 1d). However, at 120 min the inhibitor did not confer neuroprotection against OGD induced LDH release as compared to untreated slices. The LDH activity in chelerythrine chloride pre-treated OGD slices was lesser than that seen in untreated groups even in the absence of calcium.

PKC-γ and PKC-ε are Activated During OGD

As my cytotoxicity data indicated a reduction in OGD induced LDH release on PKC-γ and PKC-ε inhibition, I next investigated the effect of OGD on the expression levels of PKC-γ and PKC-ε isozymes, in particulate fractions of normoxic and ischemic slices. Redistribution of PKC from soluble to particulate fraction is considered as a marker for PKC activation. The band densities of normoxic and OGD groups in western blots were normalized against β-actin and PKC-γ and PKC-ε levels in the particulate fractions of normoxic slices were normalized to 100%. Quantitative analysis of PKC-γ isozyme levels in the particulate fractions of slices exposed to shorter durations (up to 15 min) did not result in a significant rise in total PKC-γ gamma levels compared to normoxic slices (Fig. 2a). But there was a significant enhancement in PKC-γ translocation to the particulate fractions from 15 min of OGD exposure. A maximal increase (30.62 ± 5.47%) in PKC-γ levels in the particulate fraction was seen at 60 min (Fig. 2b). However, the PKC-γ levels in particulate fraction revert back to corresponding normoxic levels at 120 min time point, suggesting a deactivation of PKC-γ from 120 min of OGD exposure. Chelerythrine chloride pre-treatment partially inhibited OGD induced PKC-γ activation (data not shown). Particulate fractions of slices exposed to shorter durations of OGD resulted in an increase (Fig. 2c) in PKC-ε translocation at 15 and 30 min (20 ± 5.64%) and (32 ± 6.34%), respectively, compared to the corresponding normoxic slices (Fig. 2d), indicating that PKC-ε is activated during OGD. The PKC-ε levels declined considerably in chelerythrine chloride pre-treated slices (not shown).

$[Ca^{2+}]_i$ Increase During OGD

Intracellular calcium overload is considered to be a crucial factor in ischemic cell death. My cytotoxicity data under calcium free conditions indicated that OGD induced cell death is calcium dependent. Hence I sought to determine the intracellular calcium changes during my experimental conditions. Fura-2 loaded slices were exposed to OGD and normoxic conditions and the rise in intracellular calcium $[Ca^{2+}]_i$, was recorded for 30 min. In normoxic slices, the basal intensity ratio (340/380 nm) was determined to be 3 ± 0.5 and this ratio remained stable for 30 min.

In slices exposed to OGD, even the basal fluorescence intensity ratio was 40.85% more than that of normoxic group. The slices showed an initial relatively rapid rise in $[Ca^{2+}]_i$ up to 10 min of exposure as evidenced by an increase in fluorescence intensity ratio, followed by a slow rise which attained a plateau later (Fig. 3a, b). The magnitude of calcium rise in OGD groups was 36% greater than that of normoxic groups at the end of 30 min.

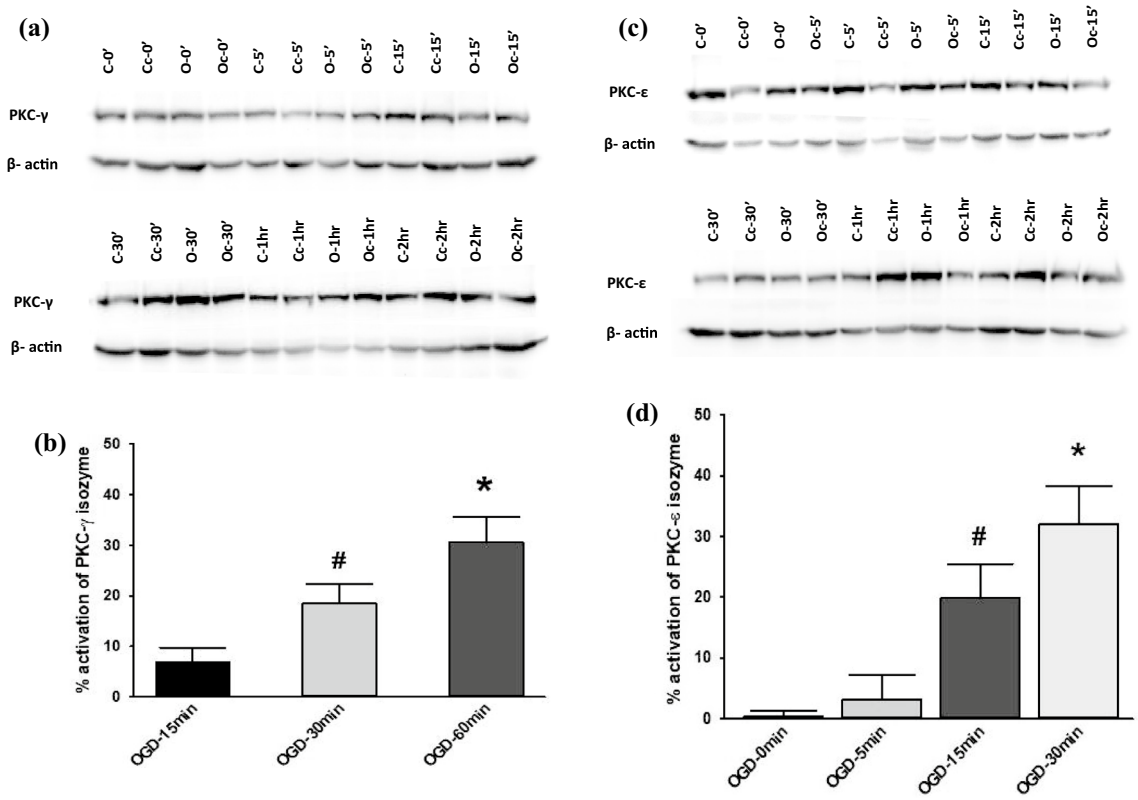

Fig. 2 Time-dependent activation of PKC-γ and PKC-ε isozymes during OGD. **a** Representative western blot of PKC-γ. 'C' represents normoxia and 'O' represents OGD experimental sets. 'Cc and Oc' represents chelerythrine chloride (10 μM) pre-treated normoxic and OGD groups respectively. **b** Quantitative analysis of PKC-γ in the blot. The band densities of PKC-γ were normalized against β-actin and presented as percent increase in PKC-γ levels with respect to normoxic group at the same time points. Data are mean ± SEM from 5 different experiments. $^{\#}P < 0.05$ and $^{*}P < 0.001$ as compared to normoxic groups. **c** Representative western blot of PKC-ε. **d** Quantitative analysis of PKC-ε in western blots. Data are mean ± SEM from 4 different experiments. $^{\#}P < 0.005$ and $^{*}P < 0.001$ as compared to normoxic groups at the same time points

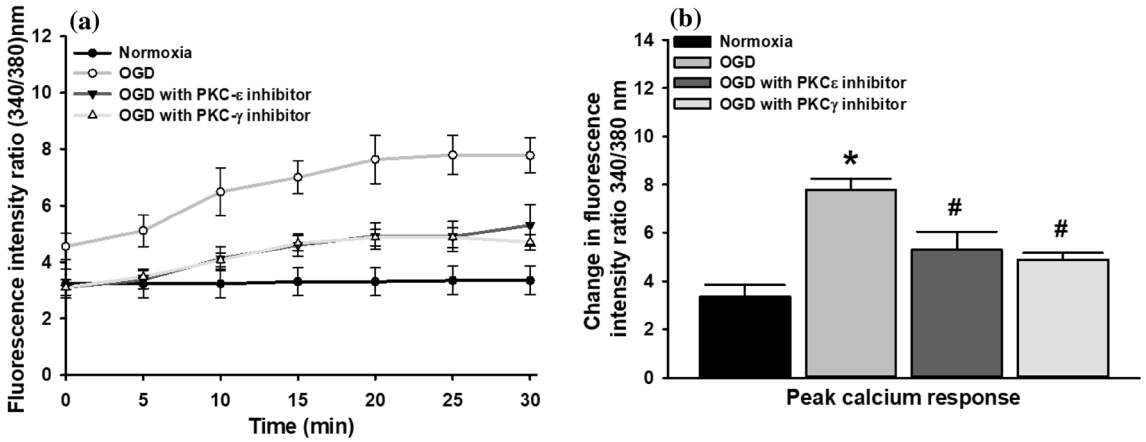

Fig. 3 Effect of PKC-ε and PKC-γ peptide inhibitors on OGD-induced intracellular calcium rise. **a** Temporal profile of OGD induced $[Ca^{2+}]_i$ rise in the presence and absence of PKC-ε and PKC-γ inhibitors (10 μM each). **b** Change in fluorescence intensity ratio 340/380 nm after 30 min of OGD exposure in PKC-ε and PKC-γ peptide inhibitor pre-treated and untreated slices. Data are mean ± SEM from five different experiments. *P and $^{\#}P < 0.001$ versus normoxic and OGD, and OGD and OGD with inhibitor groups respectively

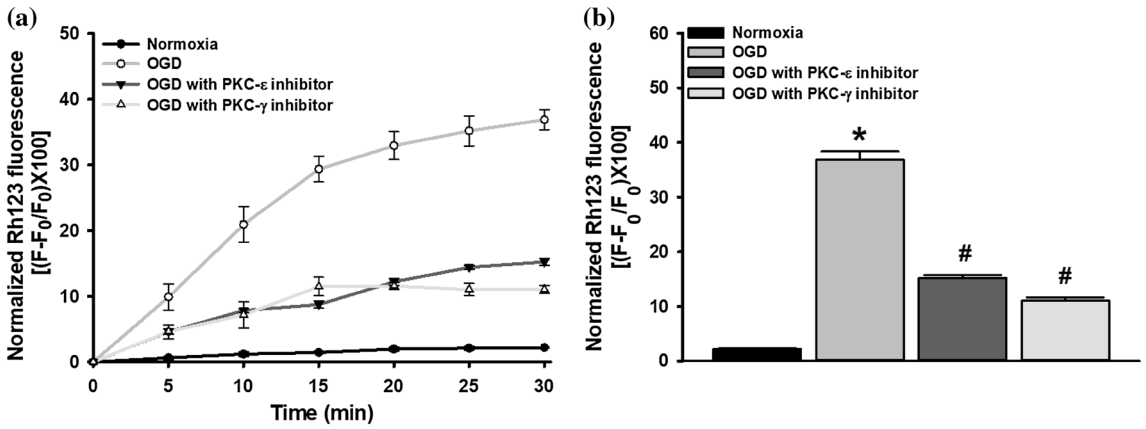

Fig. 4 Effect of PKC-ε and PKC-γ peptide inhibitors (10 μM each) on OGD-induced mitochondrial membrane depolarization. **a** Time course of OGD induced mitochondrial membrane depolarization. **b** Change in Rh123 fluorescence at the end of 30 min upon OGD exposure in PKC-ε and PKC-γ peptide inhibitor pre-treated and untreated slices. Data are mean + SEM from five different experiments. *P and $^{\#}P < 0.001$ normoxic versus OGD, and OGD versus OGD with inhibitor groups respectively

Earlier, I had observed a reduction in OGD induced LDH release when incubated in calcium-free aCSF. Hence, I carried out intracellular calcium measurements in calcium free aCSF under OGD conditions to determine whether there is any Ca^{2+} release from intracellular stores which would contribute towards the observed residual toxicity. Negligible $[Ca^{2+}]_i$ response was elicited on exposure to OGD, indicating that the increase in $[Ca^{2+}]_i$ is mainly due to Ca^{2+} influx (Fig. S5).

PKC-γ and PKC-ε Contribute to OGD-Induced $[Ca^{2+}]_i$rise

Several reports have suggested the presence of multiple isozymes of PKCs in the brain and their possible contrasting roles in mediating cellular processes. Since my cytotoxicity data in the presence of chelerythrine chloride in calcium free buffer showed a reduction in cell death I examined the involvement of PKC isozymes in OGD induced $[Ca^{2+}]_i$ raise in the presence of chelerythrine chloride. Since chelerythrine chloride was interfering with Fura-2 fluorescence the experiment could not be performed. I next tested the contribution of two specific PKC isozymes, PKC-γ and PKC-ε to OGD induced $[Ca^{2+}]_i$ rise. I found that specifically inhibiting PKC-γ and PKC-ε during OGD resulted in a marked decrease in OGD induced $[Ca^{2+}]_i$ rise (Fig. 3a). The $[Ca^{2+}]_i$ in OGD group pre-treated with PKC-γ inhibitor was attenuated by $37.16 \pm 1.19\%$ after 30 min as compared to non-treated OGD group. Pre-treatment with PKC-ε inhibitor during OGD led to a considerable reduction ($31.85 \pm 6.2\%$) in $[Ca^{2+}]_i$ response at the end of 30 min as compared to untreated OGD group (Fig. 3b).

PKC-γ and PKC-ε Inhibition Reduces OGD-Induced Mitochondrial Membrane Depolarization

Mitochondrial dysfunction is a critical determinant of ischemic neuronal injury. I studied whether mitochondrial membrane potential ($\Delta\Psi_m$) is affected under my experimental conditions. I detected that the $\Delta\Psi_m$ of normoxic slices loaded with rhodamine 123 (Rh123) did not alter significantly till 30 min. The slices exposed to OGD stress showed an initial rapid increase (17.6 fold) in Rh123 fluorescence was observed followed by a steady and continuous increase at later stage (Fig. 4a). This data suggest that mitochondrial membrane depolarizes during OGD.

To understand the effect of PKC-γ and PKC-ε in this depolarization, I individually pre-treated the slices with PKC-γ and PKC-ε specific peptide inhibitors (10 μM each) for 30 min and subjected to OGD insult. I found that in PKC-γ inhibitor treated slices, OGD exposure resulted in a decrease of $70 \pm 1.44\%$ in the extent of mitochondrial membrane depolarization at 30 min. PKC-ε inhibition during OGD resulted in an inhibition in mitochondrial depolarization by $58.69 \pm 0.69\%$ at 30 min as compared to untreated OGD slices (Fig. 4b).

PKC-γ and PKC-ε are Involved in Increased Generation of ROS During OGD

To determine the effect of OGD on reactive oxygen species formation, the rate of ROS production under normoxic and OGD conditions was assessed. I found that in DCF loaded slices exposed to OGD there was an increase in DCF fluorescence by 8.59 fold as compared to normoxic slices, indicating an increase in ROS production (Fig. 5a). To understand the roles of PKC-γ and PKC-ε isozymes in

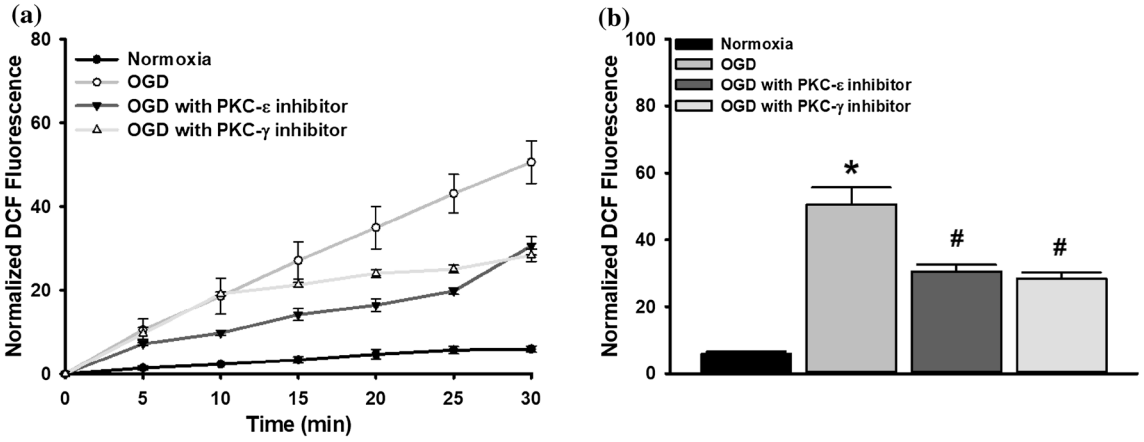

Fig. 5 Effect of PKC-ε and PKC-γ peptide inhibitors (10 μM each) on OGD-induced changes in reactive oxygen species (ROS) formation. **a** Time course of OGD induced ROS formation. **b** Change in DCF fluorescence upon OGD insult in PKC-ε and PKC-γ peptide inhibitor pre-treated and untreated slices. Data are mean ± SEM from five different experiments. *P < 0.005 between normoxic and OGD groups and #P < 0.005 between OGD and peptide inhibitor pre-treated OGD groups respectively

ROS formation during these conditions the slices were pre-treated with PKC-γ and PKC-ε peptide inhibitors prior to OGD insult and I observed that PKC-γ inhibition during OGD resulted in substantial inhibition (44.04 ± 2.92%) in ROS formation. PKC-ε inhibition under OGD too resulted in a significant reduction (39.58 ± 3.39%) in ROS formation in slices (Fig. 5b).

Discussion

Despite several investigations, it remains unclear whether PKCs mediate or are merely activated during ischemic injury [12, 13]. The present study delineates the role of PKCs in general and PKC-γ and PKC-ε isozymes in particular, in modulating the downstream events activated in response to different durations of in vitro ischemia. Experimental and clinical studies have shown that various brain areas express differential sensitivity to oxygen and/or glucose deprivation [29–31]. My cytotoxicity data showed that OGD significantly reduced slice viability as evidenced by an increase in LDH released into the extracellular medium similar to previous studies [32, 33]. There is little evidence on whether PKCs play a damaging or beneficial role during ischemia. My data showed that PKC inhibition during OGD markedly reduced cytotoxicity as evidenced by a decrease in LDH release. This clearly suggests a damaging role for PKCs in neurotoxicity during OGD. These results are consistent with earlier reports where PKC inhibition with general inhibitors protected against excitotoxic cell death in vitro and ischemic damage in vivo [13, 34]. Conversely, other studies have reported a loss of PKC activity in culture models of ischemia which correlates with neurodegenerative processes [21]. Moreover, an earlier study in primary cortical neurons showed that an early loss of membrane PKC is a necessary step in excitatory amino acid induced death [22].

Calcium is known to play a major role in downstream signaling pathways mediating ischemic injury. My experiments in calcium free aCSF showed a reduction in cytotoxicity during OGD, suggesting that neuronal death during OGD is calcium dependent to a large extent similar to an earlier report [35]. The residual toxicity observed in the absence of extracellular Ca^{2+} could be due to other factors like elevation of $[Na^+]_i$ and release of Ca^{2+} from intracellular stores and subsequent activation of downstream pathways. Further reduction in cytotoxicity on chelerythrine chloride pre-treatment suggests that PKCs still contribute towards toxicity under these experimental conditions. The PKCs involved could be the nPKCs which are $[Ca^{2+}]_i$ independent, though the role of Ca^{2+} dependent cPKCs cannot be completely ruled out as my Ca^{2+}-free experiments were conducted without emptying intracellular Ca^{2+} stores.

Mammalian brain is known to express cPKCs viz., PKC α, β, γ, and nPKCs viz., ε, δ, η and θ [36]. The overall cellular responses of PKCs result from collective actions of individual PKCs that are co-expressed in a particular cell type. Although the use of pharmacological inhibitors and activators suggested a neurotoxic role for PKCs in ischemic injury, I sought to delineate the involvement of specific PKCs in OGD. I investigated the involvement of PKC-γ, which is expressed exclusively in brain, spinal cord and retina [37] and PKC-ε, which is reported to be involved in ischemic preconditioning-induced protection in brain [13, 38]. Specific inhibition of PKC-γ or PKC-ε resulted in a marked reduction in LDH release during OGD. However, in an in vitro culture model of OGD, PKC-γ inhibition by TAT conjugated peptide (TAT- RLVLAS) showed no effect on cell survival [13].

I further assessed alterations in the expression levels of PKC-γ and PKC-ε in particulate fraction of slices following OGD. I found that PKC-γ was translocated to the particulate fraction after OGD. This pattern is suggestive of recruitment of enzymes, clearly necessary for eliciting neurotoxic/neuroprotective cell responses. In contrast to previous studies [39], I did not observe any noticeable change in PKC-γ levels in the particulate fraction during early stages of OGD. These observations lead to the conclusion that PKC-γ isoform activation may account for the deleterious processes during later stages of cerebral ischemia and its inhibition confers neuroprotection. Here, I also demonstrate the specific activation of PKC-ε in response to OGD. Even with short durations of OGD a significant increase in PKC-ε membrane translocation was observed which reverted back to corresponding normoxic levels during longer durations of OGD. Conflicting reports exist on PKC-ε activity during cerebral ischemia. Some studies report that PKC-ε is activated following OGD or in response to kainic acid treatment in in vitro and in vivo models [12, 40]. Another study in embryonic cortical culture has shown a decline in PKC-ε levels in both cytosolic and particulate fractions after OGD [13]. Other reports however, suggest that PKC-ε does not respond to ischemia/ischemia-like insults [41, 42]. These discrepancies could be attributed to differences in the duration and severity of insult in these models, cell types involved and the time points selected for assessing PKC-ε activity. Notably, many of these studies assess PKC-ε during the period of reperfusion/preconditioning. Contrary to earlier reports, my data showed that acute OGD exposure resulted in enhanced PKC-ε translocation to the particulate fraction. PKC-ε activation at very early time points during OGD suggests that this isozyme is activated following even short durations of ischemia; similar to a preconditioning stimulus. These results are consistent with studies using an organotypic hippocampal slice model in which PKC-ε is activated within 1hr following a NMDA-induced preconditioning stress, however, does not persist at 3hr post-NMDA treatment [43]. From my observations, it is likely that the activated PKC-ε may mediate the early cellular response to brief or sub-lethal ischemia, such as preconditioning. Sustained PKC-ε activation till 30 min of OGD also implies that PKC-ε activity contributes to ischemic response under severe ischemic insults. The decline in levels of both the PKCs at later stages during OGD could be due to degradation/downregulation of activated PKCs by calpains [44] or by activation of the ubiquitin/proteasome pathway [45] as occurs after prolonged PKC activation.

It is well established that calcium plays a crucial role in the pathophysiology of ischemic injury [46, 47]. PKC activation is related to cell signaling pathways involving changes in cytoplasmic Ca^{2+} levels and transmitter release in CNS neurons. My results demonstrate that there is an increase in $[Ca^{2+}]_i$ in response to OGD similar to another study on mouse layer V and layer II/III pyramidal neurons in brain [48]. Over-activation of glutamate receptors, opening of voltage-gated channels and failure of Ca^{2+} extrusion are some of the mechanisms that might cause excessive $[Ca^{2+}]_i$ accumulation under energy deprivation [49]. My data suggested an increased activity of both PKC-γ and PKC-ε during OGD, implicating them in mediating cellular response to ischemia. Inhibiting PKC-γ or PKC-ε resulted in a reduction in $[Ca^{2+}]_i$ rise during OGD, suggesting their involvement in modulating OGD induced calcium influx. The greater attenuation in $[Ca^{2+}]_i$ raise on inhibiting PKC-γ indicates a key modulatory role for this isozyme in OGD induced calcium rise. Owing to the differences in severity of the insult, the diverse mechanisms involved in calcium rise may be different. Studies have reported a role for PKCs in modulation of glutamate receptors [50, 51] as well as VGCCS [52]. Reduction in $[Ca^{2+}]_i$ raise on PKC-γ or PKC-ε inhibition during ischemia could be attributed to these facts. Earlier studies have reported a role for both calcium influx [18] and calcium release from endogenous stores [53, 54] as a contributing factor to ischemic injury. My experiments in Ca^{2+}-free aCSF showed negligible $[Ca^{2+}]_i$ rise during OGD, indicating that calcium influx is the major contributing factor to Ca^{2+} overload during OGD.

Mitochondria are cellular centers of energy production and ionic homeostasis, as well as regulators of both necrotic and apoptotic cell death [2, 3]. I observed mitochondrial depolarization during OGD. There was a complete depolarization of mitochondrial membrane during OGD as I did not observe any further depolarization with the mitochondrial uncoupler CCCP, in parallel to an earlier study conducted on substantia nigra slices [55]. Additionally, OGD is associated with cytosolic Ca^{2+} rise [56], which is sequestered by mitochondria, further contributes to $\Delta\Psi_m$ changes [57, 58]. The significant diminution in mitochondrial depolarization on specific PKC inhibition during OGD implies a role for these isozymes in modulating mitochondrial functions during ischemia. The higher attenuation in mitochondrial depolarization afforded by PKC-γ inhibitor as compared to PKC-ε could probably be due to the relatively greater reduction of calcium rise on PKC-γ inhibition. PKC-ε regulates several mitochondrial functions during ischemic preconditioning [59]. Nevertheless, PKC-ε is known to positively modulate mitochondrial channels and electron transport complexes during ischemic preconditioning [60].

Elevated $[Ca^{2+}]_i$ lead to ROS production in the neuronal cytoplasm by activating calcium dependent enzymes such as xanthine dehydrogenase, phospholipases, nitric oxide synthase, etc. and also lead to mitochondrial calcium overload [61], which results in mitochondrial damage, activation of the MPT, release of pro-apoptotic proteins, and ROS production [62, 63]. I observed higher ROS formation during OGD which could be due to the fact that ETC complexes are in a

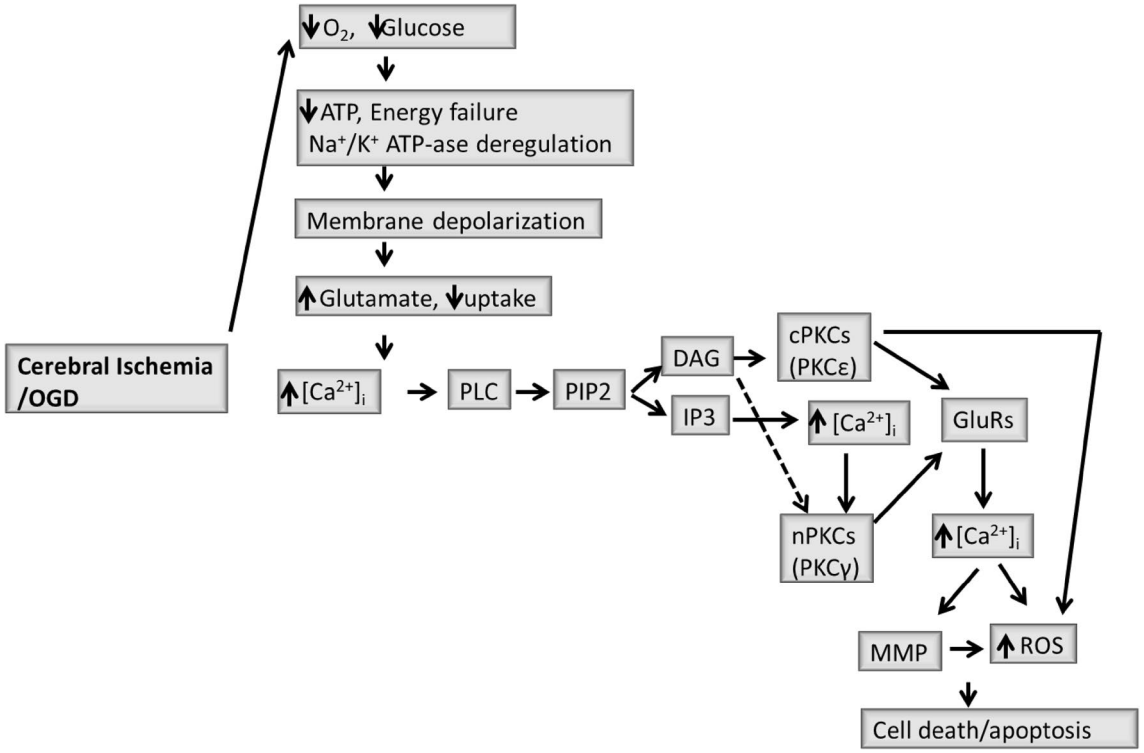

Fig. 6 A simplified schematic representation of PKC signaling in cerebral ischemia/OGD. A simplified scheme providing an overview of the important signal transduction pathways recruiting PKCs in the setting of cerebral ischemia. Due to reduced supply of oxygen and glucose during ischemia/OGD the failure of Na+-K + ATP-ase leads to membrane depolarization causing excessive release and reduced uptake of the excitatory neurotransmitter, glutamate. This leads to the excitotoxicity and subsequent neurodegeneneration where PKCs, PKCε and PKCγ play a significant role. (*PLC* phospholipase C, *PIP2* phosphatidylinositol 4,5-bisphosphate, *DAG* diacylglycerol, *IP3* inositol 1,4,5-triphosphate, *GluRs* glutamate receptors, *MMP* mitochondrial membrane potential depolarization

more reduced state during ischemia and superoxide production is favored [64]. PKC-γ or PKC-ε inhibition significantly attenuated ROS production during OGD, suggesting the role of these isozymes in modulating OGD-induced ROS generation. It has been reported that PKC-ε gets activated under hypoxic conditions and the ROS thus generated further activates PKC-γ leading to severe neuronal injury [65]. Further studies need to be conducted to address the mechanisms of these effects.

In conclusion, the current study suggests that PKC family; specifically PKC-γ and PKC-ε, contribute significantly towards OGD induced cytotoxicity. A simplified schematic overview of the important signal transduction pathways recruiting PKCs in the setting of cerebral ischemia is depicted in Fig. 6. They exhibit different activation profiles during OGD, with PKC-ε being activated earlier as compared to PKC-γ. The early PKC-ε activation during ischemia may initiate the cellular events during OGD, which followed by a delayed activation of PKC-γ would further exacerbate neuronal injury. Furthermore, my study shows that amongst the two isoforms, PKC-γ isoform contributes more towards $[Ca^{2+}]_i$ rise, mitochondrial membrane depolarization and ROS production during OGD. These isoforms may thus play pivotal central nervous system-specific roles in mediating cellular responses to ischemic insult. This study may provide implications that isozyme specific modulation of PKC activity may be a promising therapeutic route for the treatment of acute cerebral ischemic injury. Demarcating the specific signaling pathways involving PKCs, including different downstream effectors/mediators in different phases of ischemic injury will be crucial in developing PKC-based therapeutic app roaches.

Acknowledgements Support and critical comments from Nanda B. Joshi, Former Professor and, Head of the Department is highly acknowledged. This work was supported by a Research Fellowship awarded to Dayana Surendran by Council of Scientific and Industrial Research (CSIR), Government of India.

Compliance with Ethical Standards

Conflict of interest The author declares no conflict of interest.

References

1. Matsumoto S, Shamloo M, Matsumoto E et al (2004) Protein kinase C-gamma and calcium/calmodulin-dependent protein kinase II-alpha are persistently translocated to cell membranes of the rat brain during and after middle cerebral artery occlusion. J Cereb Blood Flow Metab 24:54–61. https://doi.org/10.1097/01.WCB.0000095920.70924.F5
2. Baines CP (2010) Role of the mitochondrion in programmed necrosis. Front Physiol. https://doi.org/10.3389/fphys.2010.00156
3. Newmeyer DD, Ferguson-Miller S (2003) Mitochondria Cell 112:481–490. https://doi.org/10.1016/S0092-8674(03)00116-8
4. Lan JY, Skeberdis VA, Jover T et al (2001) Protein kinase C modulates NMDA receptor trafficking and gating. Nat Neurosci. https://doi.org/10.1038/86028
5. Majewski H, Iannazzo L (1998) Protein kinase C: a physiological mediator of enhanced transmitter output. Prog Neurobiol 55:463–475. https://doi.org/10.1016/S0301-0082(98)00017-3
6. Martelli AM, Evangelisti C, Nyakern M, Manzoli FA (2006) Nuclear protein kinase C. Biochim Biophys Acta 1761:542–551. https://doi.org/10.1016/j.bbalip.2006.02.009
7. Johnson JE, Giorgione J, Newton AC (2000) The C1 and C2 domains of protein kinase C are independent membrane targeting modules, with specificity for phosphatidylserine conferred by the C1 domain. Biochemistry. https://doi.org/10.1021/bi000902c
8. Mochly-Rosen D (1995) Localization of protein kinases by anchoring proteins: a theme in signal transduction. Science. https://doi.org/10.1126/science.7716516
9. Padanilam BJ (2001) Induction and subcellular localization of protein kinase C isozymes following renal ischemia. Kidney Int. https://doi.org/10.1046/j.1523-1755.2001.0590051789.x
10. Piccoletti R, Bendinelli P, Arienti D, Bernelli-Zazzera A (1992) State and activity of protein kinase C in postischemic reperfused liver. Exp Mol Pathol. https://doi.org/10.1016/0014-4800(92)90038-D
11. Speechly-Dick ME, Mocanu MM, Yellon DM (1994) Protein kinase C: its role in ischemic preconditioning in the rat. Circ Res. https://doi.org/10.1161/01.RES.75.3.586
12. Selvatici R, Marino S, Piubello C et al (2003) Protein kinase C activity, translocation, and selective isoform subcellular redistribution in the rat cerebral cortex after in vitro ischemia. J Neurosci Res. https://doi.org/10.1002/jnr.10464
13. Wang J, Bright R, Mochly-Rosen D, Giffard RG (2004) Cell-specific role for ε- And βi-protein kinase C isozymes in protecting cortical neurons and astrocytes from ischemia-like injury. Neuropharmacology. https://doi.org/10.1016/j.neuropharm.2004.03.009
14. Domańska-Janik K, Zalewska T (1992) Effect of Brain Ischemia on Protein Kinase C. J Neurochem. https://doi.org/10.1111/j.1471-4159.1992.tb11360.x
15. Gajkowska B, Domanska-Janik K, Viron A (1994) Protein kinase C-like immunoreactivity in gerbil hippocampus after a transient cerebral ischemia. Folia Histochem Cytobiol 32:71–77
16. Felipo V, Miñana MD, Grisolía S (1993) Inhibitors of protein kinase C prevent the toxicity of glutamate in primary neuronal cultures. Brain Res. https://doi.org/10.1016/0006-8993(93)90368-W
17. Maiese K, Swiriduk M, TenBroeke M (1996) Cellular mechanisms of protection by metabotropic glutamate receptors during anoxia and nitric oxide toxicity. J Neurochem 66:2419–2428
18. Hara H, Onodera H, Yoshidomi M et al (1990) Staurosporine, a novel protein kinase C inhibitor, prevents postischemic neuronal damage in the gerbil and rat. J Cereb Blood Flow Metab. https://doi.org/10.1038/jcbfm.1990.117
19. Crumrine RC, Dubyak G, LaManna JC (1990) Decreased protein kinase C activity during cerebral ischemia and after reperfusion in the adult rat. J Neurochem. https://doi.org/10.1111/j.1471-4159.1990.tb05788.x
20. Hara H, Ayata G, Huang PL, Moskowitz MA (1997) Alteration of protein kinase C activity after transient focal cerebral ischemia in mice using in vitro [3H]phorbol-12,13-dibutyrate binding autoradiography. Brain Res 774:69–76
21. Chakravarthy BR, Wang J, Tremblay R et al (1998) Comparison of the changes in protein kinase C induced by glutamate in primary cortical neurons and by in vivo cerebral ischaemia. Cell Signal 10:291–295
22. Durkin JP, Tremblay R, Chakravarthy B et al (1997) Evidence that the early loss of membrane protein kinase C is a necessary step in the excitatory amino acid-induced death of primary cortical neurons. J Neurochem 68:1400–1412
23. Chen L, Hahn H, Wu G et al (2001) Opposing cardioprotective actions and parallel hypertrophic effects of PKC and PKC. Proc Natl Acad Sci. https://doi.org/10.1073/pnas.191369098
24. Ellrén K, Lehmann A (1989) Calcium dependency of *n*-methyl-D-aspartate toxicity in slices from the immature rat hippocampus. Neuroscience. https://doi.org/10.1016/0306-4522(89)90085-7
25. Mackay K, Mochly-Rosen D (2001) Arachidonic acid protects neonatal rat cardiac myocytes from ischaemic injury through ε protein kinase C. Cardiovasc Res. https://doi.org/10.1016/S0008-6363(00)00322-9
26. O'Donnell BR, Bickler PE (1994) Influence of pH on calcium influx during hypoxia in rat cortical brain slices. Stroke. https://doi.org/10.1161/01.STR.25.1.171
27. Sweitzer SM, Wong SME, Peters MC et al (2004) Protein kinase C epsilon and gamma: involvement in formalin-induced nociception in neonatal rats. J Pharmacol Exp Ther. https://doi.org/10.1124/jpet.103.060350.et
28. Johnson JA, Gray MO, Chen CH, Mochly-Rosen D (1996) A protein kinase C translocation inhibitor as an isozyme-selective antagonist of cardiac function. J Biol Chem. https://doi.org/10.1074/jbc.271.40.24962
29. Crepel V, Krnjevic K, Ben-Ari Y (1992) Developmental and regional differences in the vulnerability of rat hippocampal slices to lack of glucose. Neuroscience 47:579–587
30. HARA H, SUKAMOTO T, KOGURE K (1993) Mechanism and pathogenesis of ischemia-induced neuronal damage. Prog Neurobiol 40:645–670. https://doi.org/10.1016/0301-0082(93)90009-H
31. Hawker K, Lang AE (1990) Hypoxic-ischemic damage of the basal ganglia case reports and a review of the literature. Mov Disord. https://doi.org/10.1002/mds.870050306
32. Bickler PE, Hansen BM (1994) Causes of calcium accumulation in rat cortical brain slices during hypoxia and ischemia: role of ion channels and membrane damage. Brain Res. https://doi.org/10.1016/0006-8993(94)91347-1
33. Lushnikova IV, Voronin KY, Malyarevskyy PY, Skibo GG (2004) Morphological and functional changes in rat hippocampal slice cultures after short-term oxygen-glucose deprivation. J Cell Mol Med. https://doi.org/10.1111/j.1582-4934.2004.tb00279.x
34. Hong SS, Gibney GT, Esquilin M et al (2004) Effect of protein kinases on lactate dehydrogenase activity in cortical neurons during hypoxia. Brain Res. https://doi.org/10.1016/j.brainres.2004.03.004
35. Larsen GA, Berg-Johnsen J, Moe MC, Vinje ML (2004) Calcium-dependent protein kinase C activation in acutely isolated neurons during oxygen and glucose deprivation. Neurochem Res 29:1931–1937
36. Naik MU, Benedikz E, Hernandez I et al (2000) Distribution of protein kinase Mzeta and the complete protein kinase C isoform family in rat brain. J Comp Neurol 426:243–258
37. Saito N, Shirai Y (2002) Protein kinase C gamma (PKC gamma): function of neuron specific isotype. J Biochem 132:683–687

38. Di-Capua N, Sperling O, Zoref-Shani E (2003) Protein kinase C-epsilon is involved in the adenosine-activated signal transduction pathway conferring protection against ischemia-reperfusion injury in primary rat neuronal cultures. J Neurochem 84:409–412
39. Cardell M, Wieloch T (1993) Time course of the translocation and inhibition of protein kinase C during complete cerebral ischemia in the rat. J Neurochem 61:1308–1314
40. McNamara RK, Wees EA, Lenox RH (1999) Differential subcellular redistribution of protein kinase C isozymes in the rat hippocampus induced by kainic acid. J Neurochem. https://doi.org/10.1046/j.1471-4159.1999.721735.x
41. Koponen S, Kurkinen K, Åkerman KEO et al (2003) Prevention of NMDA-induced death of cortical neurons by inhibition of protein kinase Cζ. J Neurochem. https://doi.org/10.1046/j.1471-4159.2003.01846.x
42. Kurkinen K, Keinanen R, Li W, Koistinaho J (2001) Preconditioning with spreading depression activates specifically protein kinase Cdelta. Neuroreport 12:269–273
43. Raval AP, Dave KR, Mochly-Rosen D et al (2003) Epsilon PKC is required for the induction of tolerance by ischemic and NMDA-mediated preconditioning in the organotypic hippocampal slice. J Neurosci 23:384–391
44. Harada K, Maekawa T, Abu Shama KM et al (1999) Translocation and down-regulation of protein kinase C-alpha, -beta, and -gamma isoforms during ischemia-reperfusion in rat brain. J Neurochem 72:2556–2564
45. Lee HW, Smith L, Pettit GR, Smith JB (1997) Bryostatin 1 and phorbol ester down-modulate protein kinase C-alpha and -epsilon via the ubiquitin/proteasome pathway in human fibroblasts. Mol Pharmacol 51:439–447
46. Choi DW (1995) Calcium: still center-stage in hypoxic-ischemic neuronal death. Trends Neurosci 18:58–60
47. Arundine M, Tymianski M (2004) Molecular mechanisms of glutamate-dependent neurodegeneration in ischemia and traumatic brain injury. Cell Mol Life Sci 61:657–668. https://doi.org/10.1007/s00018-003-3319-x
48. Gniel HM, Martin RL (2010) Changes in membrane potential and the intracellular calcium concentration during CSD and OGD in layer V and layer II/III mouse cortical neurons. J Neurophysiol 104:3203–3212. https://doi.org/10.1152/jn.00922.2009
49. Pisani A, Bonsi P, Calabresi P (2004) Calcium signaling and neuronal vulnerability to ischemia in the striatum. Cell Calcium 36:277–284. https://doi.org/10.1016/j.ceca.2004.02.010
50. Li H-F, Mochly-Rosen D, Kendig JJ (2005) Protein kinase Cgamma mediates ethanol withdrawal hyper-responsiveness of NMDA receptor currents in spinal cord motor neurons. Br J Pharmacol 144:301–307. https://doi.org/10.1038/sj.bjp.0706033
51. Sanchez-Perez AM, Felipo V (2005) Serines 890 and 896 of the NMDA receptor subunit NR1 are differentially phosphorylated by protein kinase C isoforms. Neurochem Int 47:84–91. https://doi.org/10.1016/j.neuint.2005.04.011
52. Jonas EA, Knox RJ, Smith TC et al (1997) Regulation by insulin of a unique neuronal Ca^{2+} pool and of neuropeptide secretion. Nature 385:343–346. https://doi.org/10.1038/385343a0
53. Mattson MP, LaFerla FM, Chan SL et al (2000) Calcium signaling in the ER: its role in neuronal plasticity and neurodegenerative disorders. Trends Neurosci 23:222–229
54. Ruiz A, Matute C, Alberdi E (2009) Endoplasmic reticulum Ca(2+) release through ryanodine and IP(3) receptors contributes to neuronal excitotoxicity. Cell Calcium 46:273–281. https://doi.org/10.1016/j.ceca.2009.08.005
55. Karunasinghe RN, Lipski J (2013) Oxygen and glucose deprivation (OGD)-induced spreading depression in the Substantia Nigra. Brain Res 1527:209–221. https://doi.org/10.1016/j.brainres.2013.06.016
56. Lipski J, Park TIH, Li D et al (2006) Involvement of TRP-like channels in the acute ischemic response of hippocampal CA1 neurons in brain slices. Brain Res 1077:187–199. https://doi.org/10.1016/j.brainres.2006.01.016
57. Henrich M, Buckler KJ (2008) Effects of anoxia and aglycemia on cytosolic calcium regulation in rat sensory neurons. J Neurophysiol 100:456–473. https://doi.org/10.1152/jn.01380.2007
58. Schuchmann S, Luckermann M, Kulik A et al (2000) Ca(2+)- and metabolism-related changes of mitochondrial potential in voltage-clamped CA1 pyramidal neurons in situ. J Neurophysiol 83:1710–1721. https://doi.org/10.1152/jn.2000.83.3.1710
59. Sun X, Budas GR, Xu L et al (2013) Selective activation of protein kinase C in mitochondria is neuroprotective in vitro and reduces focal ischemic brain injury in mice. J Neurosci Res 91:799–807. https://doi.org/10.1002/jnr.23186
60. Dave KR, DeFazio RA, Raval AP et al (2008) Ischemic preconditioning targets the respiration of synaptic mitochondria via protein kinase C epsilon. J Neurosci 28:4172–4182. https://doi.org/10.1523/JNEUROSCI.5471-07.2008
61. Pivovarova NB, Stanika RI, Watts CA et al (2008) Reduced calcium-dependent mitochondrial damage underlies the reduced vulnerability of excitotoxicity-tolerant hippocampal neurons. J Neurochem 104:1686–1699. https://doi.org/10.1111/j.1471-4159.2007.05080.x
62. Starkov AA, Chinopoulos C, Fiskum G (2004) Mitochondrial calcium and oxidative stress as mediators of ischemic brain injury. Cell Calcium 36:257–264. https://doi.org/10.1016/j.ceca.2004.02.012
63. Nicholls DG (2009) Mitochondrial calcium function and dysfunction in the central nervous system. Biochim Biophys Acta 1787:1416–1424. https://doi.org/10.1016/j.bbabio.2009.03.010
64. Moncada S, Erusalimsky JD (2002) Does nitric oxide modulate mitochondrial energy generation and apoptosis? Nat Rev Mol Cell Biol 3:214–220. https://doi.org/10.1038/nrm762
65. Barnett ME, Madgwick DK, Takemoto DJ (2007) Protein kinase C as a stress sensor. Cell Signal 19:1820–1829. https://doi.org/10.1016/j.cellsig.2007.05.014